

# The Partial Renovation of Old Factory Buildings - Performance Study of the Inorganic Vitrified Micro-Bubble External Wall Insulation System

X.L. Ding & W. Shang\*

*School of Civil Architecture and Environment, Hubei University of Technology, Wuhan, Hubei 430068, China*

*\*Email: yashang3476616@163.com*

**ABSTRACT:** This paper took the partial renovation project of an old factory building in Wuhan as an example to study its external wall insulation system. A new insulation system was designed based on inorganic vitrified micro-bubbles. The material was briefly analyzed. The performance of the new insulation system was detected by designing test specimens. The results found that the specimens had favorable compressive, tensile and flexural properties, reaching the A1-level standard of construction materials, the specimens were non-combustible, and the temperature change of the concrete base was stable under the action of heating-cooling and heating-rain cycles, confirming the good insulation effect of the system. The results verify the effectiveness of the insulation system. The insulation system can be better applied in practice.

**Keywords:** old factory buildings, partial renovation, vitrified micro-bubbles, performance, thermal insulation system

## 1 INTRODUCTION

As the problem of resource shortage becomes more and more serious, the issue of energy consumption in buildings has also received ever-increasing attention (Amasyali & El-Gohary 2018), and reducing energy consumption has become an effective measure to improve energy security (Sulakatko et al. 2016). The energy consumption of buildings includes insulation, heating, ventilation and lighting (Wang & Greenberg 2015), among which insulation accounts for a large proportion. The external insulation system can improve the thermal insulation performance of a building (Sulakatko et al. 2015). It has excellent thermal insulation performance (Pedroso et al. 2020), which can stabilize the room temperature and extend the building life to achieve the purpose of energy-saving (Zhu et al. 2021). It has been more and more widely used in the renovation of buildings (Garay et al. 2017). The research on external insulation systems has become an important issue of current buildings (Yang et al. 2019). Li et al. (2017) analyzed the energy consumption on the external insulation system of a student dormitory building in Beijing. They found that the energy consumption of reinforced concrete in brick buildings was the largest, and the external insulation system with similar heat transfer coefficient but different insulation materials mainly affected the energy consumption of the material production stage. Shen et al. (2020)

studied the hydrothermal properties of external insulation systems and found that freeze-thaw and temperature drop occurred mainly in the insulation layer. Werder et al. (2015) studied the algal resistance of insulation systems, evaluated it by fluorescence and numerical analysis, and found that mineral extraction systems had higher algal resistance than organic systems. Xu et al. (2017) studied the fire performance of insulation systems and tested parameters such as mass loss and temperature. They found that the time to ignition was increased under the protection of the insulation system, and the core material was more likely to catch fire after the outer layer fell out. This study took the partial renovation of an old factory building as an example, designed its external wall insulation system, and analyzed the inorganic vitrified micro-bubble material to understand the effect of this external insulation system. This paper makes some contributions to improve the building insulation effect and promote energy saving and emission reduction.

## 2 RENOVATION OF THE EXTERNAL INSULATION SYSTEM OF OLD FACTORY BUILDINGS

### 2.1 Project introduction

The buildings of an old factory in Wuhan need to be partially renovated. In terms of “renewal of traditional office space” and based on the demand for new office space from the workforce in the context of sharing economy, this study created an island office space layout. The project site area is 3240 m<sup>2</sup>, the total construction area is 5232 m<sup>2</sup>, the greening rate is 31.2%, and the plot ratio is 1.61. The effect picture of the project is shown in Figure 1.



Figure 1. The partial renovation project for old factory buildings.

### 2.2 Design of external wall insulation system

Wuhan is characterized by hot summer and cold winter, with an annual average temperature of 15.8°C-17.5°C. In areas with hot summer and cold winter (Ruan et al. 2015), the insulation of buildings is more important. Although organic materials have good heat insulation performance, they are also flammable (Liu et al. 2015), which is unsuitable for regions with high summer temperatures. Moreover, ordinary materials are difficult to meet the demand for heat insulation and frost resistance. Therefore, our design adopts inorganic vitrified micro-bubbles in the external wall insulation system to achieve comfort and energy saving, as shown in Figure 2. Outside the base wall, a layer of interface mortar is applied first. Then, vitrified micro-bubbles insulation mortar is applied to achieve the insulation of the wall. Finally, crack-resistant mortar and mesh cloth are added outside. This is the design of the whole external wall insulation system.

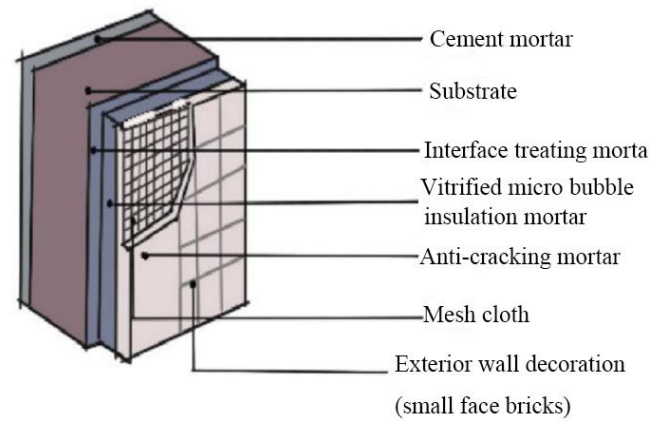


Figure 2. Design of external wall insulation system.

The vitrified micro-bubble (Hu et al. 2016) is an inorganic material with good physical properties (Zhang et al. 2018) and favorable heat insulation, sound absorption, heat preservation effects (Yu et al. 2016). Vitrified micro-bubbles avoid the high water absorption rate, empty plump and cracking of perlite and the strong inflammability and poor durability of traditional polyurethane foam; therefore, it can replace the traditional lightweight aggregates to form insulation mortar (Wang et al. 2017). It has been widely used in many projects (Su et al. 2019). In the insulation mortar, replacing the traditional aggregate (Tu et al. 2021) with vitrified micro-bubbles can effectively avoid the defects of traditional aggregate, such as easy cracking and flammability, to increase the energy efficiency of buildings (Liu et al. 2015).

### 2.3 External insulation system performance testing

#### 2.3.1 Test specimen production

Vitrified micro-bubbles (Figure 3): Xinyang Jinhualan Mining Co., Ltd. Its chemical composition is shown in Table 1, and physical properties are shown in Table 2.



Figure 3. Vitrified micro-bubbles.

Table 1. Chemical composition of vitrified micro-bubbles.

Ingredients	Mass fraction/%
SiO <sub>2</sub>	72.6
Na <sub>2</sub> O	11.8
CaO	8.1
MgO	3.4
Al <sub>2</sub> O <sub>3</sub>	2.2
Fe <sub>2</sub> O <sub>3</sub>	0.2
Other	1.7

Table 2. Physical properties of vitrified micro-bubbles.

Average particle size/ $\mu\text{m}$	60
Floating rate/%	98
Water absorption rate/%	20-50
Closed porosity/%	$\geq 95$
Pelletizing rate/%	70-90
Thermal conductivity (W/m·K)	0.032-0.045

Cement: P.O 42.5 ordinary silicate cement, Shenzhen Changhuaxin Building Material Co., Ltd.

Fiber: polypropylene fiber, Shandong Shunying Engineering Materials Co., Ltd.

Adhesive powder: building viscosity increasing instant adhesive powder, Wen'an County Jilang Building Materials Factory.

Cementing material: fly ash, Lingshou County Dingwang Mineral Products Processing Plant.

Additives: air-entraining agent and water-reducing agent, Jinan Elemental Chemical Co., Ltd.

Interface agent: Henan Yuming Coating Co., Ltd.

Anti-cracking mortar: sand as aggregate, cement as cementing material, and added with aggregates such as additives, and the sand used is from Zhangzhou Haihuan Building Materials Trading Co., Ltd.

Mesh cloth: alkali-resistant glass fiber mesh cloth, Hejian Xinhui Fireproof Insulation Material Co., Ltd.

Finish layer: flexible waterproof putty, elastic primer and topcoat, Shandong Yongmaoxin Building Materials Co., Ltd.

The process of making the concrete specimen external insulation system is as follows. The surface of the concrete specimens which have finished curing was treated to make it flat and clean; then, the interface agent was smeared evenly on the surface. After one hour of curing, the insulation mortar was smeared, and the thickness was less than 25 mm. After the surface was compacted, solidified and dried, 3 mm-thick anti-crack mortar was smeared. The grid cloth was pressed into the mortar, and the flexible putty was also smeared. The specimens were cured 24 h after the initial setting. Finally, the elastic base coat and finishing coat were smeared. The test specimen is shown in Figure 4. The wall specimens were made in the same way. Temperature sensors were arranged on the concrete base, the outer surface of the

insulation layer and the finish layer to monitor the temperature change. Three specimens were used in every group of experiment, and the results were averaged.



Figure 4. The test specimen of concrete.

### 2.3.2 Performance testing

(1) Compressive strength (Figure 5): GB/T 50081-2002 standard was referred to. A 1000 kN micro-computer-controlled electro-hydraulic servo universal testing machine (Dongguan Moujing Instrument Manufacturing Co., Ltd., China) was used. The bearing surface of the specimen was perpendicular to the top surface to maintain a balanced contact. The loading rate was 0.5-0.8 MPa/s. The loading continued until the specimen failed. The compressive strength of the specimen is:

$$f_{cc} = \frac{F}{A} \quad (1)$$

where  $F$  is the failure load and  $A$  is the pressure-bearing area.

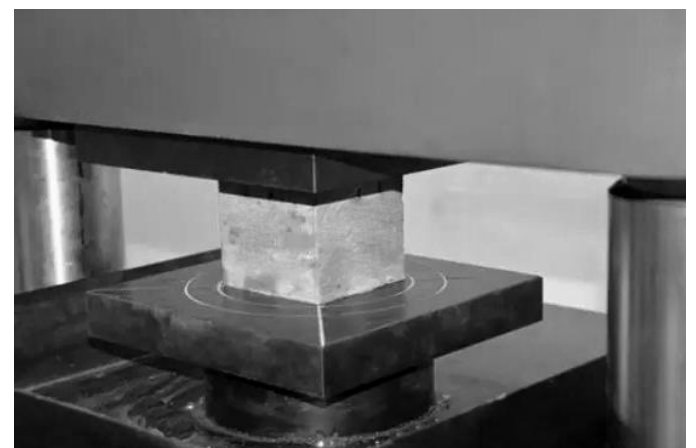


Figure 5. The test of compressive strength.

(2) Flexural strength (Figure 6): the specimen was placed in the testing machine. The method of three-point loading was used. The load was applied at a speed of 0.5-0.8 MPa/s. The loading continued until the specimen failed. The tensile strength is:

$$f = \frac{Fl}{bh^2} \quad (2)$$

where  $l$  is the span between supports and  $b$  and  $h$  are the width and height of the cross section of the test specimen.



Figure 6. The test of flexural strength.

(3) Tensile strength: the equipment used was a tensile testing machine (Cangzhou Dayong Construction Equipment Co., Ltd., China), whose loading speed was  $(5 \pm 1)$  mm/min. The load was added until the specimen failed. The flexural strength is:

$$\sigma = \frac{S_{max}}{A} \quad (3)$$

where  $S_{max}$  is the maximum tensile force and  $A$  is the cross-sectional area of the specimen.



Figure 7. The test of tensile strength.

(4) Non-combustibility: External wall insulation materials should be class A non-combustible materials. The non-combustibility of the test specimens was tested using the JT6085 building material test furnace (Shanghai Jinte Testing Equipment Co., Ltd., China) (Figure 8). The equipment used micro-computer technology to have a high degree of automation, and its top was equipped with observation mirrors to understand the burning status of the specimen. The maximum temperature in the furnace was  $900\text{ }^\circ\text{C}$ , and the temperature measurement accuracy was  $\leq \pm 0.5\text{ }^\circ\text{C}$ . The test was conducted according to GB/T 5464-2010: Non-Combustibility Test Method for Building Materials, and an electronic balance was used to measure the mass of the specimen before and after the test.



Figure 8. The non-combustibility test furnace.

(5) Weather resistance: The equipment used was the BWNH series weathering performance testing machine for external insulation system (Shenyang Weite General Technology Development Co., Ltd., China) (Figure 9). The testing machine can simulate natural environments such as high temperature and cold weather, which consists of a cooling system, a heating system, a spraying system, etc. Moreover, it is easy to operate, efficient, fully automatic, stable and relatively quiet in use.

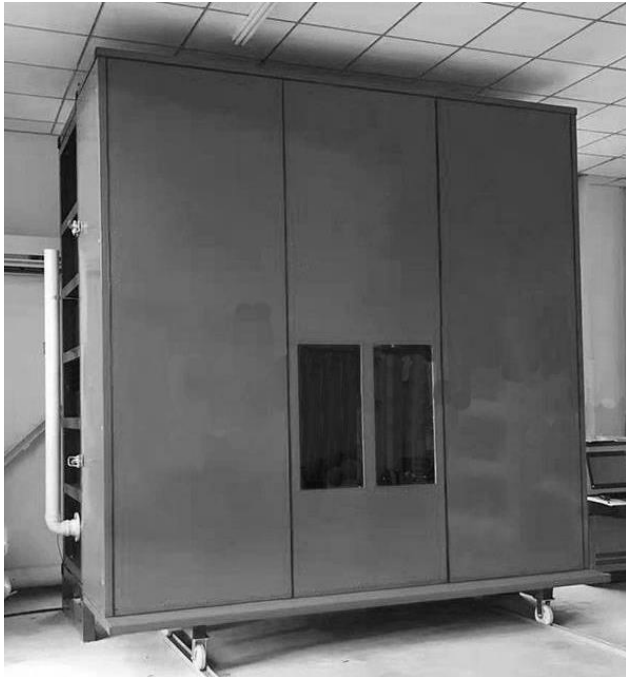


Figure 9. The weathering performance testing machine.

(6) The test consists of two parts.

① Heating-rain cycle: First, the wall specimens were continuously heated to make the surface temperature increase to 70 °C, and a constant temperature of (70 ± 5) °C was maintained. The duration of the constant temperature was not less than 1 h. Then, the specimens were drenched by water with a temperature of (15 ± 5) °C and a volume of 1-1.5L/(m<sup>3</sup>·min). Then, the test specimens were put aside for 2 h. The test was cycled 80 times.

② Heating-cooling cycle: First, the wall specimen was continuously heated to make the surface temperature increase to 50 °C, and a constant temperature of (50 ± 5) °C was maintained. The duration of the constant temperature was not less than 5 h. Then, the specimens were cooled to -20°C, and a constant temperature of (-20 ± 5) °C was maintained. The duration of the constant temperature was not less than 12 h. The test was cycled 5 times.

### 3 RESULTS AND ANALYSIS

The compressive, flexural and tensile strengths of the specimens are shown in Table 3.

Table 3. Compressive, flexural and tensile strength of wall specimens.

	Specimen 1	Specimen 2	Specimen 3	Average value
Compressive strength/MPa	35.88	36.72	35.46	36.02
Flexural strength/Mpa	5.67	5.34	5.88	5.63
Tensile strength/MPa	0.34	0.29	0.31	0.31

It was seen from Table 3 that the maximum, minimum and average compressive strength of the specimens were 36.72 MPa, 35.46 MPa, and 36.02 MPa, respectively, the maximum, minimum and average flexural strength were 5.88 MPa, 5.34 MPa, and 5.63 MPa, respectively, and the maximum, minimum and average tensile strength were 0.34 MPa, 0.29 MPa, and 0.31 MPa, respectively, indicating that the designed specimens had favorable compressive, flexural and tensile strength and could meet the requirements for use in the partial renovation of old factory buildings.

According to GB8624-2012: Classification for Burning Behavior of Building Materials and Products, the non-combustibility of the test specimens was analyzed. The results are shown in Table 4.

Table 4. Non-combustibility test results of specimens.

Standard for A1 level	Test results
Temperature rise in the furnace ≤ 30 °C	19 °C
Mass loss rate ≤ 50%	22%
Continuous burning time = 0 s	0 s

It was seen from Table 4 that the furnace temperature rise of the specimens was 19 °C, satisfying the requirement of A1-level noninflammability (≤ 30 °C); the mass loss rate of the specimens was 22%, satisfying the requirement (≤ 50%), and the continuous burning time of the specimens was 0 s, i.e., noncombustible, satisfying the requirement. Therefore, the specimens satisfied the A1-level standard, i.e., they were incombustible materials. When there are incombustible materials in the insulation system, the insulation material will not ignite under the interference of fire. In conclusion, the designed insulation system had good flame retardant and fireproof performance. In conclusion, the insula-

tion system could effectively block the spread of flame to protect personal safety.

The temperature sensor data were read to analyze the temperature variation of the insulation system, as shown in Table 5.

Table 5. Temperature variation under the heating-rain cycle.

Time /h	Concrete base/°C	Outer surface of insulation layer/°C	Finish layer/°C
0	28.64	28.79	29.01
0.5	29.33	35.67	51.26
1	34.66	48.29	57.67
1.5	35.21	49.78	58.64
2	36.78	51.26	59.21
2.5	37.11	50.98	55.63
3	38.64	50.33	54.21
3.5	36.77	46.77	50.33
4	35.83	40.39	35.67
4.5	33.65	36.92	34.33
5	33.41	33.74	33.67
5.5	33.21	32.56	33.52
6	32.67	31.27	32.88

As shown in Table 5, in the initial temperature-rise stage, with the increase of the heating time, the temperature of both the finish layer and the outer surface showed a rapid increase, and after 1 h, the temperature from the outside to the inside was 57.67 °C, 48.29 °C and 34.66 °C, respectively. In comparison, the temperature of the finish layer was the highest, with the largest temperature-rise amplitude (28.66 °C), followed by the outer surface of the insulation layer (19.5 °C), and the temperature-rise amplitude of the concrete base was the smallest, only 5% compared to the initial temperature. The above results demonstrated that the designed insulation system had the effect of heat insulation, effectively preventing the rapid temperature rise. In the constant-temperature stage, the temperature of the finish layer was maintained around 60 °C, the temperature of the outer surface was about 55 °C, and the temperature of the concrete base had a slow increase but was always below 40 °C. The above results suggested that the insulation system could effectively control temperature and keep the room temperature constant, ensuring good comfort. Then, in the spraying stage (3 h - 4 h), the finish layer's temperature rapidly declined from about 55 °C down to about 35 °C under the action of water; the insulation layer was less affected due to the indirect effect of water, and the amplitude of reduction was smaller than the finish layer, from 50 °C to about 40 °C; the temperature reduction of the concrete base was slower under the joint action of the finish and insulation layers, only about 5 °C, suggesting that the insulation system could maintain stable temperatures in case of sudden changes in external temperature. Fi-

nally, after spraying, the temperature variation of the specimens tended to be stable. In general, the temperature of the concrete base layer was relatively stable under the protection of the insulation system, with an overall fluctuation amplitude of about 10 °C, and did not fluctuate too much due to the change of external temperature.

The temperature variation of the insulation system under the heating-cooling cycle is shown in Table 6.

Table 6. Temperature variation under the heating-cooling cycle.

Time /h	Concrete base/°C	Outer surface of insulation layer/°C	Finish layer/°C
0	23.64	24.05	24.12
1	28.66	36.88	70.12
2	29.36	38.99	69.87
3	31.22	40.12	68.99
4	33.97	42.64	65.46
5	35.64	45.33	63.77
6	37.21	47.88	64.21
7	39.25	48.69	63.96
8	41.22	50.12	63.27
9	38.76	23.26	19.24
10	35.64	20.69	-5.12
11	30.29	15.34	-10.68
12	25.64	10.67	-14.36
13	20.38	5.32	-18.65
14	15.67	-0.84	-18.96
15	14.32	-2.36	-19.03
16	13.27	-4.67	-19.16
17	12.68	-5.12	-19.36
18	11.28	-6.89	-19.57
19	11.06	-7.94	-19.62
20	10.97	-9.12	-19.77
21	10.86	-10.03	-19.89
22	10.64	-10.29	-19.97
23	10.41	-10.31	-20.03
24	10.29	-10.34	-20.12

It was seen from Table 6 that in the initial temperature-rise stage, with the increase of the heating time, the temperature of the finish layer increased rapidly and soon reached about 70 °C, the temperature of the outer surface grew fast but was slower than the finish layer, with a variation amplitude of about 10°C, and the temperature of the concrete base changed the least, about 5°C. Subsequently, in the constant-temperature stage, the ambient temperature was maintained at (50 ± 5) °C, the temperature of the finish layer began to drop to about 60 °C (a reduction of about 10 °C), the temperature of the outer surface was maintained at about 50 °C after a slow rise, and the temperature of the concrete base layer rose to about 40 °C. Then, under the effect of cool-

ing, the temperature of the specimen showed a significant drop, the temperature of the finish layer had dropped to about  $-5\text{ }^{\circ}\text{C}$  (a reduction of about  $70\text{ }^{\circ}\text{C}$ ), the temperature of the outer surface was around  $20\text{ }^{\circ}\text{C}$ , and the temperature of the concrete base was around  $30\text{ }^{\circ}\text{C}$ , which showed the smallest decrease amplitude. The above results suggested that the insulation system maintained the temperature of the concrete base layer well and prevented it from being affected by the sudden drop of the external temperature. In the final constant-temperature stage, the temperature of the finish layer remained stable after dropping to about  $-20\text{ }^{\circ}\text{C}$ , the temperature of the insulation layer dropped to about  $-10\text{ }^{\circ}\text{C}$ , and the temperature of the concrete base stabilized at about  $10\text{ }^{\circ}\text{C}$  after a slow drop. In the case of a sudden drop of  $70\text{ }^{\circ}\text{C}$  in the outside temperature, the temperature of the concrete base only dropped by about  $30\text{ }^{\circ}\text{C}$ . Overall, the concrete base was able to maintain the temperature despite the sharp drop in outdoor temperature, and the overall drop was about  $30\text{ }^{\circ}\text{C}$ , verifying the thermal insulation performance of the system.

#### 4 CONCLUSION

This paper studied the external insulation system in the partial renovation of the old factory building. The project adopted the inorganic vitrified micro-bubble external wall insulation system. Various properties of the test specimens were analyzed through design and detection. The results showed that the compressive, flexural and tensile strength of the specimens were  $36.02\text{ MPa}$ ,  $5.63\text{ MPa}$ , and  $0.31\text{ MPa}$ , respectively. The non-combustibility test found that the specimens satisfied the A1-level standard, i.e., they were noncombustible. The heating-cooling and heating-rain cycles found that the insulation system could maintain the temperature of the concrete base layer in a stable state even when the external temperature dropped suddenly.

In conclusion, the inorganic vitrified micro-bubble external wall insulation system performed well in various aspects and could satisfy the needs of partial renovation of old factory buildings. The inorganic vitrified micro-bubble external wall insulation system can be promoted and applied in actual engineering projects to strengthening building insulation and reduce energy consumption.

#### 5 REFERENCES

Amasyali, K., and El-Gohary, N. M., "A review of data-driven building energy consumption prediction studies", *Renewable & Sustainable Energy Reviews*, Vol. 81, No. pt.1, January 2018, pp 1192-1205.

- Garay, R., Arregi, B., and Elguezal, P., "Experimental Thermal Performance Assessment of a Prefabricated External Insulation System for Building Retrofitting", *Procedia Environmental Sciences*, Vol. 38, 2017, pp 155-161.
- Hu, C., Li, H., Liu, Z., and Wang, Q., "Research on Properties of Foamed Concrete Reinforced with Small Sized Glazed Hollow Beads", *Advances in Materials Science and Engineering*, Vol. 2016, January 2016, pp 1-8.
- Liu, Y. J., Hai, H., Fan, L. M., and Zhang, J. W., "Review and Prospect of Study on External Vertical Fire Spread up High Rise Buildings in China", *Advanced Materials Research*, Vol. 1065-1069, December 2015, pp 2328-2332.
- Liu, Y., Wang, W., Zhang, Y., and Li, Z., "Mechanical properties of thermal insulation concrete with a high volume of glazed hollow beads", *Magazine of Concrete Research*, Vol. 67, No. 13-14, July 2015, pp 1-14.
- Li, Y., Gong, X., Zhang, Q., and Shi, C. Q., "Energy Consumption Analysis of Building with Typical External Thermal Insulation System", *Materials Science Forum*, Vol. 898, No. pt.3, July 2017, pp 1970-1977.
- Pedroso, M., Flores-Colen, I., Silvestre, J. D., Gomes, M. G., Silva, L., Sequeira, P., and de Brito, J., "Characterisation of a multilayer external wall thermal insulation system. Application in a Mediterranean climate", *Journal of Building Engineering*, Vol. 30, July 2020, pp 101265.
- Ruan, F., Qian, X., Zhu, Y. T., Wu, M. L., Qian, K. L., and Feng, M. P., "Wall Insulation Effect on Building Energy Efficiency with the Intermittent and Compartmental Energy Consuming Method", *Applied Mechanics & Materials*, Vol. 744-746, March 2015, pp 2340-2347.
- Shen, X., Li, L., Cui, W., and Feng, Y., "Thermal and Moisture Performance of External Thermal Insulation System with Periodic Freezing-thawing", *Applied Thermal Engineering*, Vol. 181, No. 5, November 2020, pp 115920.
- Sulakatko, V., Lill, I., and Liisma, E., "Analysis of On-site Construction Processes for Effective External Thermal Insulation Composite System (ETICS) Installation", *Procedia Economics and Finance*, Vol. 21, No. 8, 2015, pp 297-305.
- Sulakatko, V., Lill, I., and Witt, E., "Methodological Framework to Assess the Significance of External Thermal Insulation Composite System (ETICS) on-site Activities", *Energy Procedia*, Vol. 96, September 2016, pp 446-454.
- Su, Z., Guo, L., Zhang, Z., and Duan, P., "Influence of different fibers on properties of thermal insulation composites based on geopolymer blended with glazed hollow bead", *Construction and Building Materials*, Vol. 203, No. APR.10, April 2019, pp 525-540.
- Tu, J., Wang, Y., Zhou, M., and Zhang, Y., "Heat transfer mechanism of glazed hollow bead insulation concrete", *Journal of Building Engineering*, Vol. 40, No. 2, August 2021, pp 102629.
- Wang, L., and Greenberg, S., "Window operation and impacts on building energy consumption", *Energy & Buildings*, Vol. 92, No. apr., April 2015, pp 313-321.
- Wang, W., Liu, Y., Li, Z., Zhao, L., and Chen, Y. F., "Calculation on effective thermal conductivity of recycled aggregate thermal insulation concrete with added glazed hollow beads", *Materialprüfung*, Vol. 59, No. 2, February 2017, pp 202-209.
- Werder, J. V., Venzmer, H., and Cerny, R., "Application of fluorometric and numerical analysis for assessing the algal resistance of external thermal insulation composite systems", *Journal of Building Physics*, Vol. 38, No. 4, 2015, pp 290-316.
- Xu, L., Zhou, Y., Li, K., Liu, C., and Cheng, X., "Experimental study on fire behaviors of external thermal insulation composite system under vertical radiation", *Fire & Materials*, Vol. 41, No. 7, May 2017, pp 826-833.

- Yang, Z. H., Guo, P. L., Chen, X., and Jiang, W., "Heat and humidity performance of EPS and Rock wool board external thermal insulation system", *IOP Conference Series Materials Science and Engineering*, Vol. 592, September 2019, pp 012008.
- Yu, L., Zhang, C., and Wu, Z. G., "Preparation and Performance of Inorganic Thermal Insulation Glazed Hollow Bead Material", *Key Engineering Materials*, Vol. 680, February 2016, pp 306-310.
- Zhang, Y., Ma, G., Wang, Z., Niu, Z., Liu, Y., and Li, Z., "Shear behavior of reinforced glazed hollow bead insulation concrete beams", *Construction & Building Materials*, Vol. 174, No. JUN.20, June 2018, pp 81-95.
- Zhu, K., Jiang, W., Yu, L., Guo, P., and Yang, Z., "Deformation analysis and failure prediction of bonding mortar in external thermal insulation cladding system (ETICS) by coupled multi physical fields method", *Construction and Building Materials*, Vol. 278, No. 8, April 2021, pp 122017.